

# Cortex-wide topography of 1/f-exponent in Parkinson's disease

Pascal Helson \*<sup>1</sup>, Daniel Lundqvist<sup>2</sup>, Per Svenningsson<sup>3</sup>, Mikkel C. Vinding<sup>\*2,4</sup>, and Arvind Kumar<sup>\*1</sup>

<sup>1</sup>*School of Electrical Engineering and Computer Science, KTH Royal Institute of Technology, Stockholm, Sweden and Science for Life Laboratory, Sweden*

<sup>2</sup>*Department of Clinical Neuroscience, NatMEG, Karolinska Institutet, Stockholm, Sweden*

<sup>3</sup>*Section of Neurology, Department of Clinical Neuroscience, Center for Molecular Medicine, Karolinska Institutet, Stockholm, Sweden. Karolinska Hospital, Stockholm, Sweden*

<sup>4</sup>*Copenhagen University Hospital - Hvidovre, Copenhagen, Denmark*

## Abstract

Parkinson's Disease causes progressive and debilitating changes to the brain as well as to the mind. While the diagnostic hallmark features are the characteristic movement-related symptoms, the disease also causes decline in sensory processing, cognitive, emotional performance and most patients develop dementia over time. The extent of symptoms and the brain-wide projections of neuromodulators such as dopamine suggest that many brain regions are simultaneously affected in Parkinson's disease. To characterise such disease-related and brain-wide changes in neuronal function, we performed a source level analysis of resting state magnetoencephalogram (MEG) from two groups: Parkinson's disease patients and healthy controls. Besides standard spectral analysis, we quantified

---

\*Corresponding authors: [pashel@kth.se](mailto:pashel@kth.se), [mikkelcv@drcmr.dk](mailto:mikkelcv@drcmr.dk), [arvkumar@kth.se](mailto:arvkumar@kth.se)

the aperiodic component of the neural activity by fitting a power law ( $\kappa/f^\lambda$ ) to the MEG spectrum and then studied its relationship with age and UPDRS. Consistent with previous results, the most significant spectral changes were observed in the high theta/low alpha band (7-10 Hz) in all brain regions. Furthermore, analysis of the aperiodic part of the spectrum showed that, in all but frontal regions,  $\lambda$  was significantly larger in Parkinson's disease patients than in control subjects. Our results indicate for the first time that Parkinson's disease is associated with significant changes in population activity across the whole neocortex. Surprisingly, even early sensory areas showed a significantly larger  $\lambda$  in patients than in healthy controls. Moreover,  $\lambda$  was not affected by the L-dopa medication. Finally,  $\lambda$  was positively correlated with patient age but not with UPDRS-III (summary measure of motor symptoms' clinical rating). Because  $\lambda$  is closely associated excitation-inhibition balance, our results propose new hypotheses about manifestation of Parkinson's disease in cortical networks.

**Running title:** 1/f-exponent in Parkinson's disease

**Keywords:** Parkinson's disease, MEG, aperiodic activity, cortex-wide, excitation-inhibition balance.

**Abbreviations:** PD = Parkinson's disease, BR = brain region, MDS-UPDRS = Movement Disorder Society's Unified Parkinson's Disease Rating Scale, EI = excitation-inhibition, BG = basal ganglia, FC = functional connectivity, HC = healthy control, PSD = power spectral density.

## 1 Introduction

2 In Parkinson's Disease (PD), the progressive loss of the dopaminergic cells not only depletes the  
3 neuromodulator dopamine but also alters the dynamics of other key neuromodulators such as sero-  
4 tonin, noradrenaline and acetylcholine (see the review by McGregor and Nelson<sup>1</sup>). Given the  
5 widespread prevalence of neuromodulators in the neocortex, it is expected that the neocortical neu-  
6 ral circuits dynamics and function would also be affected in PD. That is, the signature of PD related  
7 dysfunction should also be visible in the neuronal activity recorded from neocortical regions.

8 Consistent with this, analyses of EEG and MEG have revealed several changes in the population  
9 activity of different neocortical regions (see reviews by Geraedts et al.<sup>2</sup> and Boon et al.<sup>3</sup>). While  
10 the results are diverse given the heterogeneity of the patients, it is commonly observed that the low  
11 frequency – delta to low-alpha band – power increases whereas high-alpha to gamma band power  
12 decreases.<sup>4</sup>

13 This kind of spectral slowing was shown to be correlated with motor and cognitive symptoms.<sup>5</sup>  
14 Such spectral slowing has been observed in the earliest stages of the disease (e.g. in the posterior  
15 cortex regions<sup>6</sup>), hence demonstrating that it is not an effect of dopamine medication. Moreover,  
16 dopamine replacement therapy hardly reverses the spectral slowing, especially in the more ad-  
17 vanced PD patients.<sup>6</sup>

18 Spectral power alterations are also associated with changes in functional connectivity (FC) in  
19 PD patients. Throughout the disease, the low-alpha band FC decreases after an initial increase.<sup>7,8</sup>  
20 Increase in beta band synchrony is also commonly observed in the basal ganglia as well as in the  
21 cortico-basal ganglia loops (see the review by Hammond et al.<sup>9</sup>).

22 Thus, previous work on analysis of EEG/MEG has been largely focused on oscillatory activity  
23 in different frequency bands. Besides oscillations, the aperiodic part of the population activity  
24 can also be informative about the underlying network dysfunction and relative excitation-inhibition  
25 balance.<sup>10</sup> To the best of our knowledge, the aperiodic part of the EEG/MEG activity in PD was  
26 characterised in three studies. First, Vinding et al.<sup>11</sup> reported steeper power law decay of MEG

27 power in sensorimotor regions of PD patients. In a more recent study, Wiesman et al.<sup>12</sup> estimated  
28 the aperiodic activity on four different frequency bands showing a neurophysiological slowing –  
29 decrease through frequency of the  $\lambda$  deviation from HC. Finally, Wang et al.<sup>13</sup> studied low-spatial  
30 resolution EEG from PD-ON and OFF medication showing that there is a significant increase of  
31 the offset and exponent power law parameters from OFF to ON medication in some of the sensors.  
32 However, thus far it has remained unclear how the spatial distribution of aperiodic component of  
33 the population activity is altered by chronic dopamine depletion and dopamine replacement therapy  
34 in human patients.

35 Therefore, we studied the spatial distribution of spectral peaks and aperiodic component of the  
36 activity from neural populations measured with MEG in PD patients in their on and off medication  
37 states. To this end, MEG acquired using 306 sensors were pre-processed to obtain 44 sources'  
38 activity distributed all over the neocortex according to the HCP-MMP1 atlas. We found that indeed  
39 there is a slowing in the MEG spectrum even when the spectral peaks were identified without  
40 classical frequency band definition. Analysis of the power-law exponent ( $\lambda$ ) of MEG spectrum  
41 revealed a significant increase in the  $\lambda$  in sensory and motor regions in PD patients compared to  
42 the healthy controls. In fact,  $\lambda$  showed a spatial positive gradient from anterior to posterior brain  
43 regions in PD patients. Surprisingly, the frontal regions which receive most of the dopaminergic  
44 projections did not show a significant difference in  $\lambda$ . L-dopa administration did not affect the  
45 spatial distribution of  $\lambda$ . However,  $\lambda$  changes were correlated to the patients' age but not to their  
46 UPDRS-III score (the clinical rating of motor symptoms). That is, neocortical activity dynamics  
47 is more vulnerable to chronic dopamine changes in older PD patients than in younger patients.  
48 Moreover, our results reveal aspects of neocortical population activity which are not affected by the  
49 L-dopa therapy. Because 1/f-exponent ( $\lambda$ ) can be linked to excitation inhibition (EI) balance, our  
50 analysis suggests new testable hypotheses about the PD related changes in the neocortex.

## 51 Materials and methods

### 52 MEG data and its pre-processing

53 Here we analysed the resting state (eyes opened) MEG recorded from 17 PD patients (age 41-  
54 85; five female) and 20 age matched healthy controls (HC; age 54-76; eight female). The data was  
55 acquired at the Swedish National Facility for MEG (NATMEG, <https://natmeg.se/>) using the Elekta  
56 Neuromag TRIUX 306-channel MEG system. The study was approved by the regional ethics  
57 committee (Etikpöingsnöamden Stockholm, DNR: 2016/911-31/1) and followed the Declaration  
58 of Helsinki. All participants gave written informed consent before participating.

59 For more details of the experimental protocol please refer to Vinding et al.<sup>14</sup> study. Briefly, the  
60 MEG was acquired at a sampling rate of 1 kHz with an online 0.1 Hz high-pass filter and 330 Hz  
61 low-pass filter. Each subject was recorded twice. MEG from PD patients was recorded in OFF  
62 and ON medication states. In the OFF medication condition, PD patients were off their dopamine  
63 replacement medications (Levodopa) for at least 12 hours. After the first recording session, patients  
64 took their medication and MEG was recorded for the second time one hour after the medication  
65 intake. HC subjects were also recorded twice at an interval of 1 h.

66 Each recording epoch was of 8 minutes duration. Data were down-sampled to a sampling fre-  
67 quency of 200 Hz and a low pass filtered at 45 Hz was applied. We pre-processed the data to re-  
68 move non-neural noise and eye movement artifacts using ICA and data from electro-oculogram or  
69 electrocardiogram. We then used the dynamic statistical parametric mapping (dSPM<sup>15</sup>) for source  
70 reconstruction (implemented in MNE-Python<sup>16</sup>), followed by a labelling using HCP MM1 atlas<sup>17</sup>  
71 which resulted in 44 brain regions (BR) signals as shown in Figure 1.

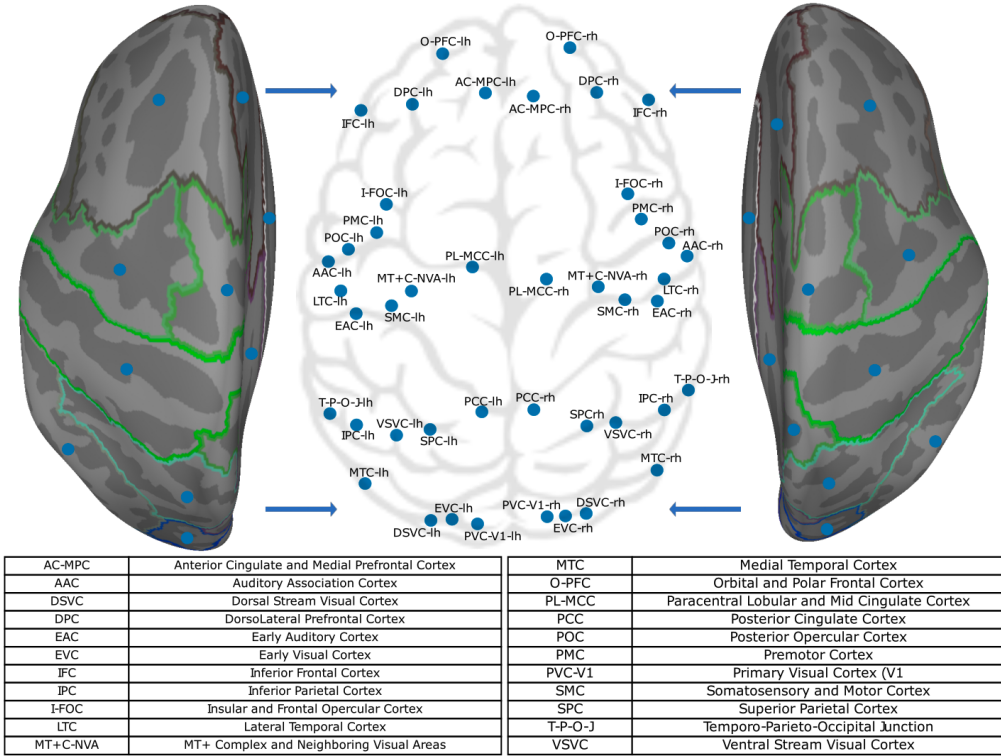


**Figure 1: Cortex-wide projection of the centre of mass of the 44 brain regions investigated here using MEG.** The brain regions were extracted using the HCP MM1 atlas.

## 72 Extraction of the frequency peaks

73 For each BR of each patient we estimate the power spectral density (PSD) – using the Welch  
 74 method<sup>18</sup> implemented in SciPy `citescipy` with default parameters (average = 'mean' and window  
 75 = 'hann') – averaging over 5 sec segments with 50% overlap over the whole signal. The periodic  
 76 part of the spectrum was extracted using the FOOOF method proposed by Donoghue et al.<sup>19</sup>.

77 FOOOF optimally fits the PSD with a function composed of the sum of an aperiodic part and a  
 78 periodic part. The aperiodic part is modelled as  $\frac{\kappa}{f^\lambda}$  where  $f > 0$  Hz is the frequency,  $\kappa$  is the offset  
 79 of the PSD and  $\lambda$  defines how the PSD decays as a function of  $f$ . The periodic part is modelled as a  
 80 sum of  $P$  weighted Gaussian distributions whose mean, standard deviation and weight respectively  
 81 indicate the peak frequency, width and height of the spectral power bump of the peak. We manually

82 specified the frequency band (1-45 Hz) on which the fitting was done. To identify oscillatory peaks  
83 in the PSD using FOOOF, we need to provide the maximum number of peaks  $P$ , their minimum  
84 height and band width. We searched for  $P = 4$  peaks with a minimum peak height of  $10^{0.2} \text{ V}^2/\text{Hz}$   
85 and peak width within [1, 10] Hz (see Figure 2 C).

86 From the proportion of individuals having such peaks within each group, we defined a nor-  
87 malised difference between groups as

$$D_{prop}^{band}_{PD\ OFF-HC}(b) = \frac{p_{PD\ OFF}^{band}(b) - p_{HC}^{band}(b)}{p_{PD\ OFF}^{band}(b) + p_{HC}^{band}(b)}$$

88 where  $p_G^{band}(b)$  is the proportion of individual in the group  $G \in \{PD\ OFF, HC\}$  having at least  
89 one peak frequency in the frequency band  $band$  and the brain region  $b$  (see Figure 4 B). These  
90 proportions,  $p_G^{band}(b)$ , for the theta and gamma frequency bands are illustrated in Figure 4 C and D,  
91 respectively.

## 92 Temporal dynamics of the slope of the MEG power spectrum

93 To characterise the aperiodic component of the MEG activity, we focused on the way the power  
94 of the MEG signals decayed as a function of the frequency. To this end, we first estimated the  
95 time-resolved spectrum (spectrogram) of each MEG source (epoch size = 50 sec, overlap 40 sec,  
96 see Figure 2 A). The PSD for each epoch was evaluated using Welch's method averaging over 2 sec  
97 segments with 50% overlap (default parameters: average = 'mean' and window = 'hann'). Next,  
98 we fitted a power law to each PSD using the FOOOF algorithm. In the aperiodic activity analysis,  
99 we used the frequency band [1, 45] Hz, a minimum peak height of  $10^{0.2} \text{ V}^2/\text{Hz}$ , a peak width within  
100 [2, 10] Hz and a maximum of 4 peaks (see Figure 2 C for an example of such a FOOOF fitting).  
101 Finally, we obtained the temporal and spatial dynamics of  $\lambda$ ,  $\kappa$  and  $P$  by applying this method  
102 to each epoch of each source (see Figure 2 D red trace). We checked the accuracy of the fit by  
103 computing its r-squared error (for all the data combined; mean: 0.94, standard deviation: 0.04).

## 104 Calibration of $\lambda$ estimate

105 *A priori* it is not clear how much error is expected in the estimation of  $\lambda$  given a specific  $\lambda$  and  
106 epoch size. We have fixed the epoch size to 50 sec, which is large enough to give us a good  
107 estimate of the PSD. Still we need to determine the appropriate segment size ( $W$ ) for Welch's  
108 algorithm. To address this issue we resorted to a numerical simulation approach. First, we created  
109 a PSD of the form  $\frac{\kappa}{f^{\lambda_{true}}}$ , and assigned random phase (drawn from a uniform distribution  $\mathcal{U}_{[-\pi, \pi]}$ )  
110 to each frequency. Next, we used inverse Fourier transform to reconstruct a signal of desired  
111 length (Figure S1 A). Finally, we extracted  $\lambda_{sim}$  for different values of  $W$  (Figure S1 D-F). We  
112 systematically varied  $\lambda_{true}$  and  $W$ . We found that the error in the estimate of  $\lambda_{sim}$  depends on  
113 both the  $\lambda_{true}$  and  $W$  (Figure S1 E,F). Based on these numerical experiments we chose  $W = 2$  sec.  
114 which gave us the best compromise between the errors in mean and standard deviation of the  $\lambda$  in  
115 a range that we have observed in our data.

## 116 Variability of $\lambda$

117 For each brain region, we assume that  $\lambda$  depends only on two parameters, time and group (PD  
118 patient ON or OFF medication and HC). So, for a brain region  $b$  and a subject  $i$ ,  $\lambda_i^b(t)$  is the typical  
119 dynamics of the 1/f-exponent. To estimate the variability of  $\lambda_i^b(t)$  as a function of time in a given  
120 individual and BR, we calculated the coefficient of variation (CV) as:

$$CV_i^b = \frac{\sigma_{\lambda_i^b}}{\bar{\lambda}_i^b},$$

121 where  $\sigma_{\lambda_i^b}$  and  $\bar{\lambda}_i^b$  are respectively the standard deviation and the mean of  $\lambda_i^b(t)$ .

## 122 Relationship between $\lambda$ and subject age and UPDRS-III scores

123  $\lambda$  could be related to the subject age and disease severity (UPDRS-III score) in both linear or  
124 non-linear manner. Therefore, we estimated both linear and non-linear measures of dependence  
125 between  $\lambda$  and  $x \in \{age, UPDRS\}$  using the following three descriptors:

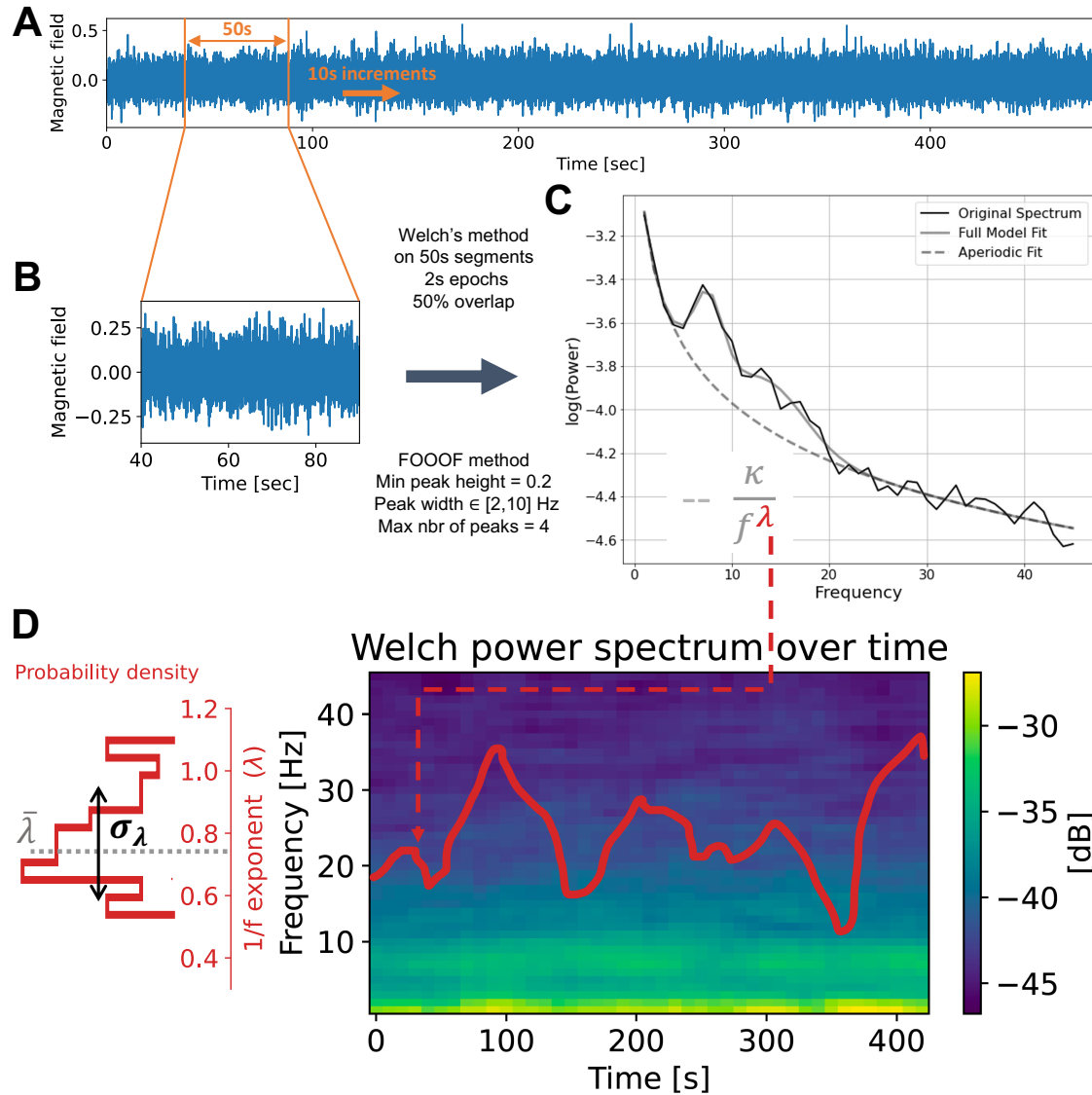


**Figure 2: Overview of the estimation of  $\lambda$  dynamics done on every BR of each patient.** (A) Time series of MEG from a source located in the pre-motor cortex left hemisphere of a PD patient. (B) Zoom in one epoch (duration 50 sec) of the time series of Panel A. (C) The black line shows the PSD of the time series of panel B. The gray line is the full fit provided by FOOOF package. The dotted line shows the aperiodic activity following a power law  $\frac{\kappa}{f^\lambda}$ . (D) Right: Pseudocolor image of the PSD as a function of time. The red line shows the corresponding  $\lambda$  for each epoch. Left: Temporal probability density of  $\lambda$ .

- 126 • *Distance correlation* measures the non-linear dependence between two variables:

$$d_{cov}(\lambda, x) = \frac{1}{n^2} \sum_{j,k} (a_{jk} - \bar{a}_k - \bar{a}_j + \bar{a}) (b_{jk} - \bar{b}_k - \bar{b}_j + \bar{b})$$

127 where using the notation  $\|\cdot\|$  for the Euclidean norm,

$$a_{jk} = \|\lambda_j - \lambda_k\|, b_{jk} = \|x_j - x_k\|, \text{ and } \forall c \in \{a, b\}, \bar{c}_j = \frac{1}{n} \sum_k c_{jk}, \bar{c} = \frac{1}{n} \sum_j \bar{c}_j.$$

128 Here  $\lambda_i$  refers to the slope of the frequency spectrum of  $i^{th}$  subject for a given brain region.

129 Other variables and this definition are illustrated in Figure 3. For further details please see  
130 the work by Székely et al.<sup>20</sup>.

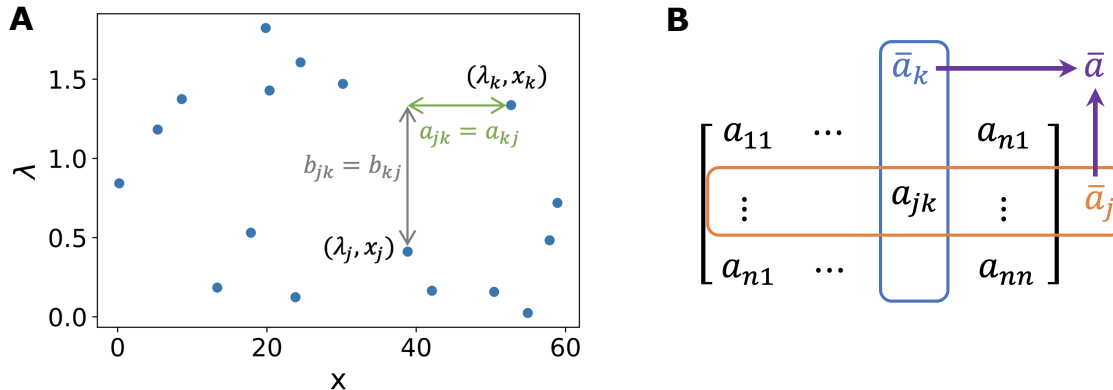


**Figure 3: Schematic of distance correlation measurement.** (A) Example of a sample of  $(\lambda, x)$  in a given brain region for 17 different individuals (uniformly drawn).  $(a_{ml})_{m,l}$  (resp.  $(b_{ml})_{m,l}$ ) is the matrix of distances within the vector  $\lambda$  (resp.  $x$ ). (B) Computations on  $(a_{ml})_{m,l}$  rows and columns:  $\bar{a}_j$  is the mean of the  $j^{th}$  row (or column as  $(a_{ml})_{m,l}$  is symmetric) and  $\bar{a}$  is the mean of  $(\bar{a}_j)_j$ .

- 131 • *Pearson correlation* measures the linear link between two variables:

$$\rho(\lambda, x) = \frac{cov(\lambda, x)}{\sigma_\lambda \sigma_x},$$

132 where  $cov$  is covariance and  $\sigma_x$  is the standard deviation of the variable  $x$ .

- 133 • *Spearman correlation* measures the monotonic relationship between two variables:

$$r_s(\lambda, x) = \rho(R(\lambda), R(x))$$

134 where  $R(\cdot)$  is the rank function.

135 To disentangle the dependence of  $\lambda$  on the age and UPDRS-III, we computed the partial correlations.  
136 To do so, we used *partial\_corr* function of the *pingouin* Python package to calculate the  
137 Pearson and Spearman partial correlations. Concerning the partial distance correlation, it is similar  
138 to the classical partial correlation. It is based on projections but now in a more complex space called  
139 the Hilbert space of U-centred matrices. We refer to the work by Székely and Rizzo<sup>21</sup> for a rigor-  
140 ous definition. We used the corresponding function, *partial\_distance\_correlation*, from the Python  
141 package *dcor*<sup>21</sup> for more information). We performed a permutation test (200 000 permutations on  
142 the  $x$  variable) to estimate the p-values.

## 143 Statistical tests

144 With the exception of the correlations among UPDRS-III, age and  $\lambda$ , we used the Kolmogorov-  
145 Smirnov test from the *ks\_2samp* function implemented in SciPy to determine the statistical signif-  
146 icance of our results. This test captures more the deviations near the distribution centre than at its  
147 tails. Moreover, its power is greater when used in the one-tailed case. Therefore, we used the latter  
148 to test whether the cumulative distribution functions (CDFs) of one variable is greater or less in  
149 one group compared to another. In the test, the statistic is  $D^+ = \sup_{u \in \mathbb{R}} [F(u) - G(u)]$  where  $F$   
150 and  $G$  are the CDFs to be compared.<sup>22</sup> For example, when comparing the  $\bar{\lambda}$  in Figure 5 B, we tested  
151 whether the CDF of  $\bar{\lambda}_{PD OFF}$  was less than  $\bar{\lambda}_{HC}$  in the frontal regions and the opposite in other BRs.  
152 When comparing the two HC groups – between sessions 1 and 2, see Figure S2 B –  $\bar{\lambda}_{HC \ ses1}$  and  
153  $\bar{\lambda}_{HC \ ses2}$  are statistically closed (distributions across the group) so that we gathered both groups as  
154 one group (the HC group). However, the CVs difference between the two sessions was of the same  
155 order than the difference between the CVs of HC and PD-OFF or PD-ON medication. Thus, we  
156 only compared CVs session-wise: PD-OFF and HC ses1, PD-ON and HC-ses2, see Figure S2 C,D.

157 Concerning the statistical significance of correlation measures, we performed a permutation test  
158 (200 000 permutations on the  $x$  variable) to estimate the p-values of the partial distance correlation.  
159 For Pearson and Spearman partial correlations, two-sided p-values were computed from the one-

160 sample *t*-test. The degrees of freedom of this test is  $N - 1$  where  $N$  is the data size ( $N = 17$  in PD  
161 groups and  $N = 20$  in healthy groups).

162 Finally, we did not correct for multiple comparisons. We only used comparison-wise error rate  
163 for each specific brain area, because this study is an exploratory work on the possible changes of  
164 the 1/f-exponent dynamics in PD. The alpha-level that was used to determine significance was a  
165 p-value less than 0.01. However, as we performed statistical tests on 44 BRs, a p-value of less than  
166  $0.05/44 \sim 0.001$  has a significance level of 0.05 after Bonferroni correction, which is the most  
167 conservative correction for multiple comparison.

## 168 Data availability

169 The MEG data cannot be made publicly available because of the ethical permits. The data analysis  
170 scripts are available at: [https://github.com/paschels/PD\\_one\\_over\\_f](https://github.com/paschels/PD_one_over_f).

## 171 Results

172 To characterise how cortical activity is changed in human PD patients, we analysed the MEG  
173 signals acquired during resting state. To this end, we quantified both the oscillatory peaks and the  
174 slope of the spectrum for MEG sources corresponding to 44 different brain regions and then we  
175 estimated the dependence of the latter on age and UPDRS-III.

## 176 Frequency slowing in PD

177 Analyses of MEG and EEG from PD patients suggest that frequency associated with peak power in  
178 theta and alpha bands is reduced in human PD patients when compared to healthy controls.<sup>3</sup> To test  
179 whether this is also the case in our data, we searched for Gaussian peaks in the spectrum of MEG  
180 signals without explicitly defining the frequency bands (see Materials and methods).

181 By estimating the distribution of all the frequency peaks observed across all the brain regions,  
182 we found that indeed in PD there is a general slowing of spectral peaks (PD-PFF vs HC, p-value

183     $< 10^{-20}$  with Kolmogorov-Smirnov test, see Figure 4 A). Notably, Levodopa medication did not  
184    improve this slowing, in fact, if at all it seemed to worsen the frequency slowing (PD-PFF vs PD-  
185    ON, p-value < 0.017 with Kolmogorov-Smirnov test).

186    Next, we sorted the frequency peaks into classical frequency bands (theta = 4-8 Hz, alpha = 8-  
187    13 Hz, beta = 13-30 Hz and gamma = 30-45 Hz). Thus, we obtained the proportion of peak fre-  
188    quency ( $p_G^{band, b}$ ) for each *band*, MEG source *b* and group *G*. Given the spectral slowing there were  
189    not enough peaks in the theta and gamma bands to compare the HC and PD groups (Figure 4 A).  
190    Therefore, first we restricted our analysis to alpha and beta bands. Even though there was a re-  
191    duction in alpha band peak power, the difference did not reach a statistical significance level for  
192    none of the brain regions (Figure 4 B, left). In the beta band also we found a wide spread decrease  
193    in the mean peak frequency among most of the patients. However, the difference was statistically  
194    significant in only one brain region (Figure 4 B, right). This suggests that spectral slowing does not  
195    affect the alpha and beta bands locally. However, when we pool data across all the brain regions,  
196    spectral slowing can be observed in all bands. The main local effect (i.e. brain region specific) of  
197    spectral slowing is the reduction in the power of gamma band oscillations and increase in the power  
198    of theta bands oscillations. In particular, gamma band peaks were almost completely missing from  
199    the frontal regions in PD patients (Figure 4 D). By contrast, HC seem to be lacking theta band peaks  
200    in the central-temporal and posterior brain regions (Figure 4 C).

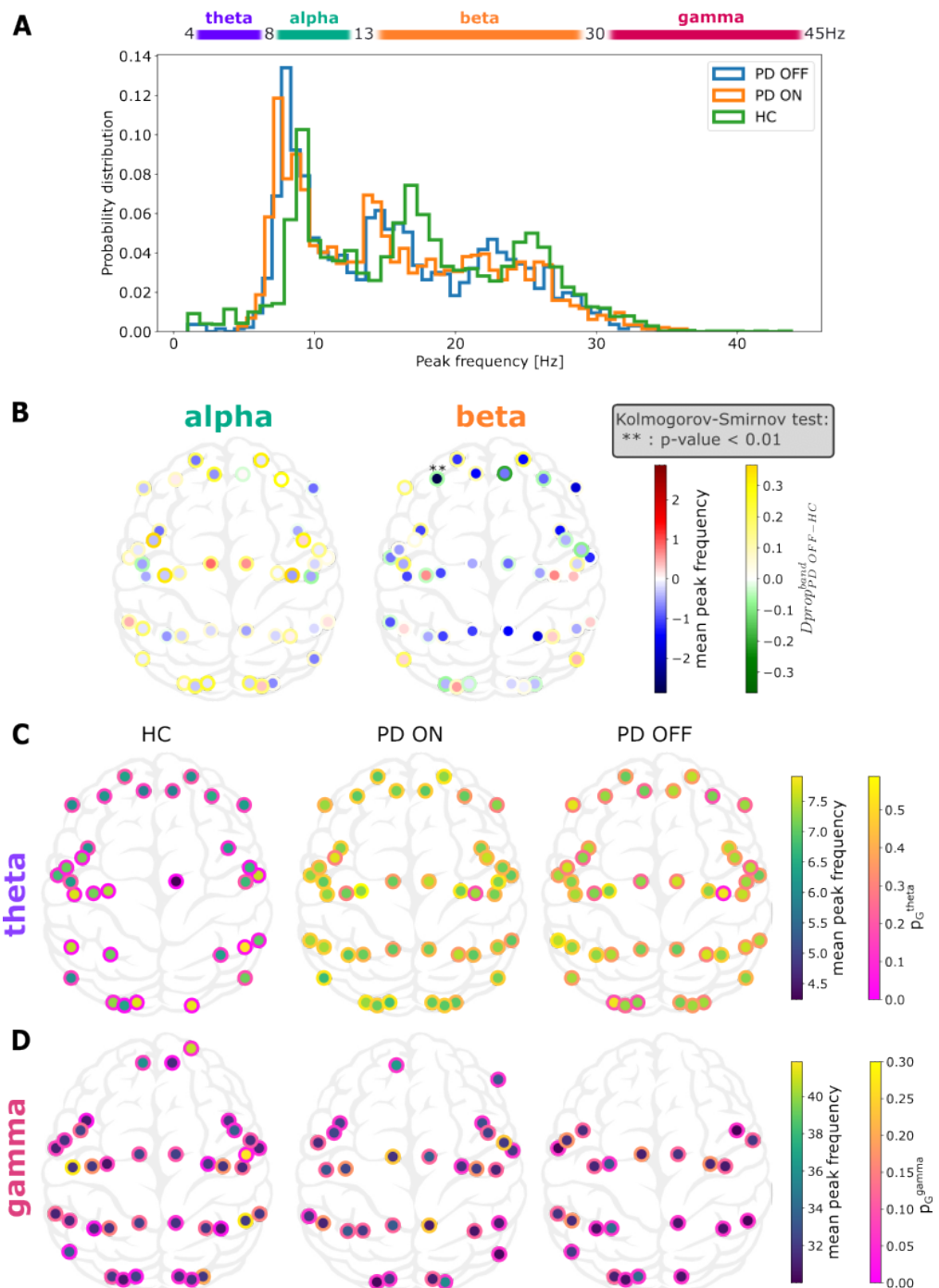


**Figure 4: Spectral slowing, a peak frequency perspective.** (A) Distribution of peak frequencies in all BRs of all individuals from the different groups. (B) Distribution of frequency peaks in alpha and beta bands. The colour inside the dots is the difference (PD-PFF - HC) of the mean peak frequency of each brain region in alpha (left) and beta (right). The edge colour of the dots is the normalised difference (PD-PFF - HC) of proportion of individuals having at least one peak frequency in the given band. (C, D) Distribution of frequency peaks in theta (C) and gamma (D) bands. Dot colour indicates mean peak frequency within the theta (C) and gamma (D) band. Edge colour of the dots indicate the proportion of individuals having such peaks in the given group.

## 201 Neocortex-wide change in the 1/f-exponent distribution in PD

202 Next, we focused on the aperiodic component of the neural activity and analysed how the spectral  
203 power decreased as a function of frequency. Using the FOOOF algorithm we fitted a power law  
204 function to the PSD (see Materials and methods) and estimated the exponent  $\lambda$  for each MEG source  
205 and subject. Across all the data,  $\lambda$  spanned a relatively wide range 0.1-2.0. However, temporal  
206 variation of  $\lambda$  for individual brain regions in both healthy controls and PD patients was smaller  
207 than across subject variance (Figure 5 A,B). We found that in healthy controls,  $\lambda$  was smaller in  
208 sensory regions than in the cognitive regions (Figure 5 C, left). However, this apparent gradient of  
209  $\lambda$  from frontal to posterior regions is not statistically significant.

210 By contrast, in PD patients (both OFF and ON medication)  $\lambda$  was larger in sensory regions  
211 than in the cognitive regions (Figure 5 C, middle, right). Moreover,  $\lambda$  showed a clear frontal to  
212 posterior gradient (Spearman correlation, p-value  $< 10^{-6}$  and  $r_s(\bar{\lambda}_G^b, y^b) < -0.65$  where  $y^b$  is the  
213 y-coordinate of the BR  $b$  and  $G \in \{PD\ OFF, PD\ ON\}$ ).

214 From Figure 5 C, it is clear that there are differences in the spatial distribution of  $\lambda$  in PD patients  
215 and HC. To quantify this difference, we performed a brain region wise comparison of  $\lambda$  in HC  
216 and PD patients OFF medication (Figure 5 D right). We found that PD patients (OFF medication)  
217 have larger  $\lambda$  in auditory, visual, somato-senssory and motor regions than in HC (for significant  
218 figures please see Figure 5 D right). The same landscape of differences in  $\lambda$  was observed when we  
219 compared PD patients ON medication with HC (Figure 5 D middle). Interestingly, a comparison  
220 of PD patients in ON and OFF medication states did not reveal any significant differences across  
221 the whole neocortex (Figure 5 D left). We also note that still in most brain regions (except frontal  
222 areas), the group variance among HC was much lower than among PD patients (edge colours of  
223 the dots in Figure 5 C). Finally, the most significant changes were observed in the left hemisphere,  
224 which is expected as in our cohort most patient's disease started in their right hand.

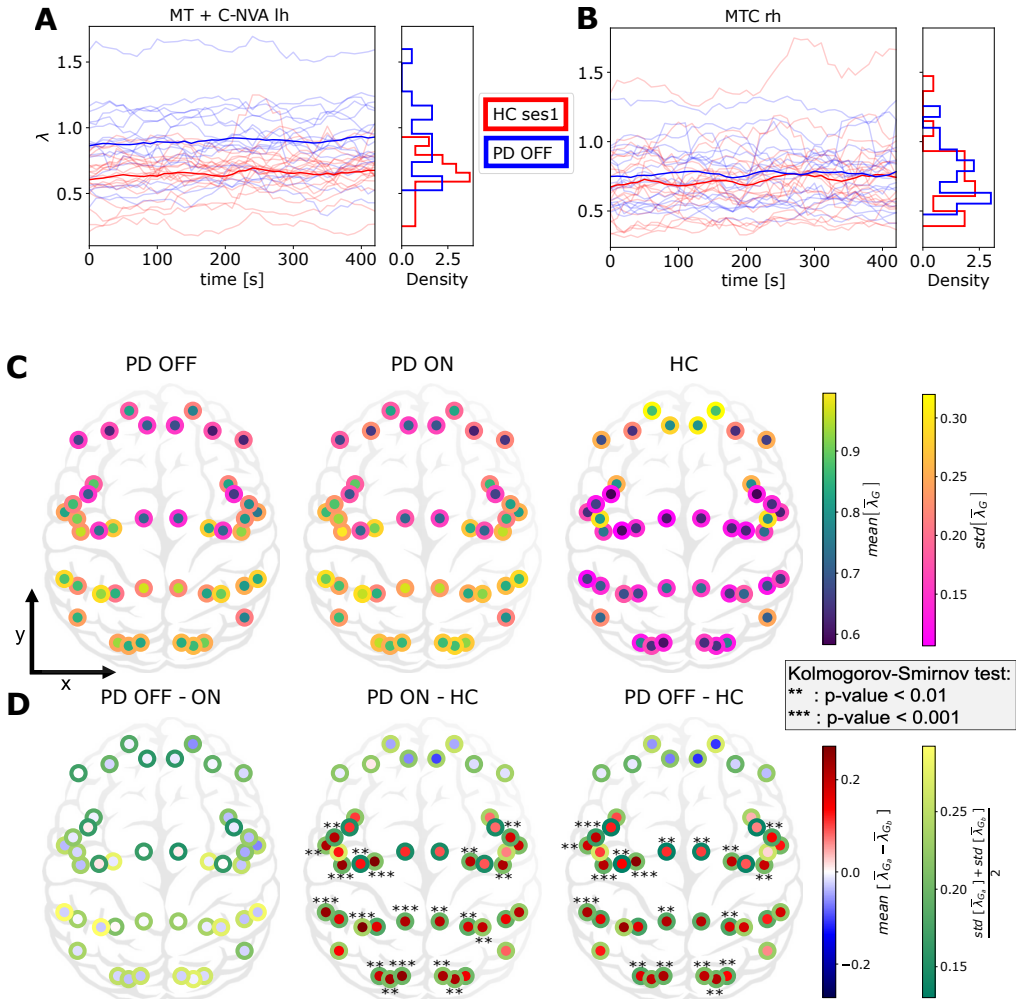


**Figure 5: Cortex-wide distribution of the mean over time of  $\lambda$  within each group.** (A, B) Temporal evolution of  $\lambda$  over time in two specific regions (MT+C-NVA-lh and MTC-rh) for PD patients OFF medication (pale blue) and HC (pale red). Each line corresponds to one subject. Blue and red lines indicate group averages. (C) Temporal average of  $\bar{\lambda}_G$  for each group  $G \in \{\text{HC, PD-ON, PD-PFF}\}$ . The inside colour refers to the mean over the group. The border colour refers to the fluctuation of  $\bar{\lambda}_G$  within the group  $G$ . (D) Temporal average of  $\lambda$  between two groups  $G_a, G_b \in \{\text{HC, PD-ON, PD-PFF}\}$ . The inside colour refers to the difference between the means over the groups. The border colour refers to the averaged fluctuation of  $\bar{\lambda}$  combining the two groups  $G_a$  and  $G_b$ .

225         $\lambda$  is not constant across time (Figure 5 A,B). To quantify these fluctuations over time, we mea-  
 226        sured the coefficient of variation (CV, see Materials and methods) of  $\lambda$  for each BR in each subject.

227 Small value of CV of  $\lambda$  indicates temporal stability of  $\lambda$ . In general  $\lambda$  was stable over time (small  
228 CV). However,  $\lambda$  was more variable in frontal regions in both PD patients and HC (Figure S2 C).  
229 A comparison of CV of PD patients and HC revealed that for most brain regions  $\lambda$  was less vari-  
230 able in PD patients than in HC, particularly in the sensory regions where the CV difference was  
231 statistically significant (Figure S2 D,right).

232 Finally, even if there is no significant difference in this second order temporal statistics between  
233 PD patients ON and OFF medication, Levodopa seems to decrease temporal fluctuations in some  
234 BRs, especially frontal ones (Figure S2 D,left).

## 235 **The 1/f-exponent is positively correlated with age but not with UPDRS- 236 III in PD**

237 In the above we have shown how  $\lambda$  was altered in PD patients across the whole neocortex. The  
238 question arises: does this difference in  $\lambda$  also correlate with the PD severity?  $\lambda$  could be affected  
239 by subject age and UPDRS-III score. Therefore, we estimated partial correlations between  $\lambda$  and  
240 UPDRS-III given age, and age given UPDRS-III for each brain region separately.

241 We found that a negative partial correlation between  $\bar{\lambda}$  and UPDRS-III scores but these correla-  
242 tions do not reach a statistical significance level (Figure 6 A, see also Figure S4 for Spearman and  
243 Pearson correlations). On the other hand, in PD patients (both ON and OFF medication),  $\bar{\lambda}$  and age  
244 were positively correlated, especially in the left hemisphere T-P-O-J, SPC, PCC, MTC, MT + C-  
245 NVA, I-FOC, EAC, DSVC and LTC, VSVC in the right hemisphere (Figure 6 B, see also Table 1 for  
246 BR names, Table S1 for exact p-values and Figure S3 for Spearman and Pearson correlations). By  
247 contrast, we did not find any significant correlation between  $\bar{\lambda}$  and age in healthy controls. Despite  
248 a decline in the dopaminergic neuron function due to normal ageing,<sup>23</sup> these “normal” changes do  
249 not seem sufficient to affect the aperiodic component of cortical population activity, unlike in PD.

250 It is somewhat counter intuitive that despite significant PD-related changes in  $\bar{\lambda}$ , it was not cor-  
251 related with UPDRS-III, even in the motor regions of the cortex. This result may be explained by  
252 a lack of sensitivity of the data or by the fact that  $\bar{\lambda}$  is not by itself related to motor symptoms.

253 The fact that the increase in  $\bar{\lambda}$  was positively correlated with age suggests that persistent dopamine  
 254 depletion may be more detrimental for brain networks that are already undergoing age related de-  
 255 terioration like the sensory areas. For instance, vision is impaired in PD, especially in patients with  
 256 cognitive decline.<sup>24,25</sup> Alternatively, brain networks in the younger patients may be more malleable  
 257 to compensate for the loss of dopamine than in older patients.

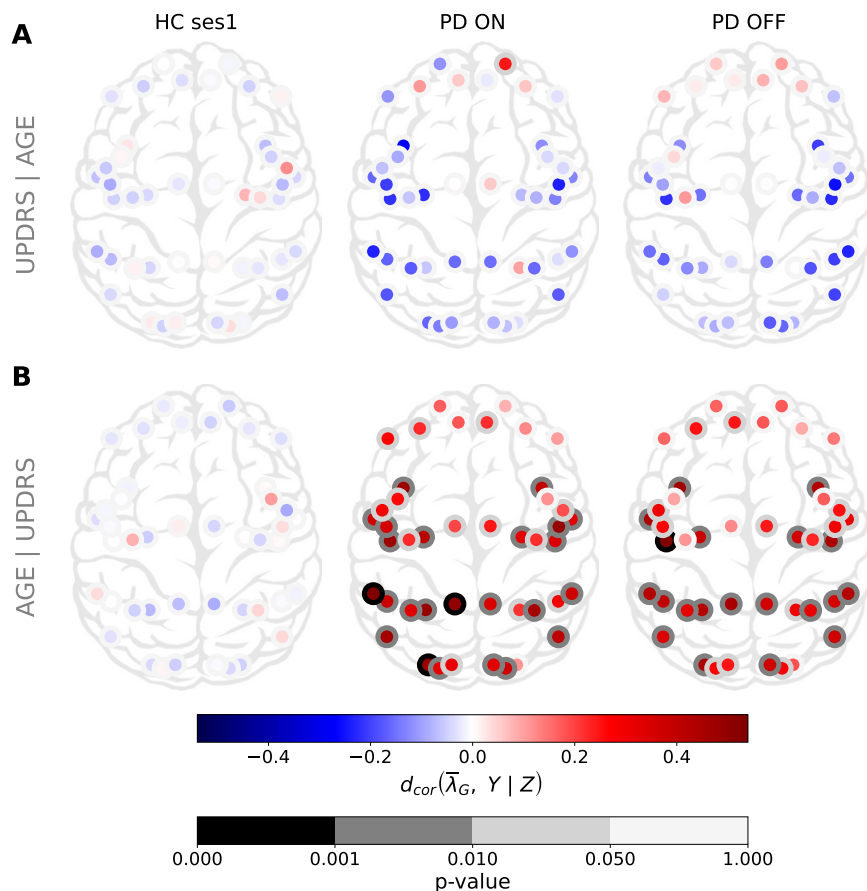


**Figure 6: Cortex-wide distribution of partial distance correlation between the mean over time of  $\bar{\lambda}_G$  and  $Y$  knowing  $Z$  for each group  $G \in \{HC \text{ ses1}, PD \text{ ON}, PD \text{ OFF}\}$ . (A)  $(Y, Z) = (\text{UPDRS}, \text{age})$ . (B)  $(Y, Z) = (\text{age}, \text{UPDRS})$ .**

## 258 Discussion

259 Given chronic change in the neuromodulator dopamine we expect that excitation and inhibition  
260 (EI) balance may be altered in the neocortical regions. To test we analysed the aperiodic activity  
261 of MEG data which has been inversely related to EI balance in several previous studies.<sup>26-35</sup> We  
262 found that the 1/f-exponent ( $\lambda$ ) was higher in PD patients than in HC in most brain regions but  
263 not in frontal regions. The most significant changes occurred within sensory and motor regions.  
264 Moreover, we found that  $\lambda$  showed a spatial gradient from posterior to anterior brain regions in PD  
265 patients. Although not significant, in HC the gradient of  $\lambda$  was reversed compared to that in the  
266 PD patients. When examining the fluctuations of  $\lambda$  over time, we found that  $\lambda$  was more variable  
267 in the frontal regions. Moreover,  $\lambda$  fluctuated more in HC controls than in PD patients. This was  
268 not expected as  $\lambda$  was globally larger in PD. Surprisingly, l-dopa medication had a little effect on  
269 the topography of  $\lambda$ . Finally, we computed different correlation measures between  $\lambda$  and both the  
270 age and UPDRS-III score. We did not find any correlations in the HC group neither with age or  
271 UPDRS-III. Although not significant, global negative correlations with UPDRS-III were observed  
272 in PD patients. On the other hand,  $\lambda$  was positively correlated with age in PD patients in both ON  
273 and OFF medication states.

274 Previously, Vinding et al.<sup>36</sup> analysed the same data for 1/f slope ( $\lambda$ ) but that analysis was re-  
275 stricted to the sensorimotor association regions. Consistent with our results, they also found that  $\lambda$   
276 was positively correlated with age in PD patients but not in HC and the correlation between  $\lambda$  and  
277 UPDRS-III was not significant. We build on that study and now show the topography of  $\lambda$  over the  
278 whole neocortex in both healthy controls and PD patients. Our analysis shows that  $\lambda$  changes in  
279 early sensory regions are also correlated with age but only in PD patients.

280 Recently, Wang et al.<sup>13</sup> analysed the 1/f slope of EEG activity. Our results differ from their re-  
281 sults in several ways. First, concerning the topography of  $\lambda$ 's topography, we found that  $\lambda$  decreased  
282 (increased) from sensory to cognitive regions in PD patients (healthy controls). By contrast, Wang  
283 et al.<sup>13</sup> have reported similar topography in both healthy and PD patients. In their study,  $\lambda$  was high

284 in the central regions with a decrease in all directions from there on. This difference might be due  
285 to the fact that we used a brain atlas to project the MEG sensors to sources. Moreover, we have a  
286 much denser spatial sampling of the space using 306 MEG sensors as opposed to the 32 EEG sen-  
287 sors used by Wang et al.<sup>13</sup>. However, this is a conspicuous difference that should be investigated in  
288 a study where both MEG and EEG are acquired from the same patients. In contrast to Wang et al.<sup>13</sup>,  
289 we did not find significant differences between PD-ON and PD-OFF states. This could be due to  
290 the difference in recording protocols in the two studies: in our case, dopamine effects were acute in  
291 the sense that patients were OFF medication for at least 12 hours but then took the medication only  
292 one hour before the ON medication state was recorded. Unlike Wang et al.<sup>13</sup>, we have analysed  
293 partial correlation between UPDRS-III/age and each MEG source. This separation of brain regions  
294 and partial correlation revealed that  $\lambda$  was correlated to age but only in PD patients.

## 295 Interpretation of 1/f slope

296 There are at least three possible interpretations of the changes in  $\lambda$ . Population signals such as  
297 MEG are generated by dipoles created by transmembrane currents.<sup>37</sup> The transmembrane currents  
298 are generated due to synaptic inputs impinging on the neurons. Therefore, the frequency spec-  
299 trum of the MEG (and also EEG, LFP) reflects the time constants of the synaptic inputs. Typically,  
300 inhibitory (GABAergic) synaptic transients have a longer time constant than excitatory (glutamater-  
301 gic) current. Therefore, increased  $\lambda$  may be an indicator of either increased GABAergic or reduced  
302 glutamatergic currents. That is,  $\lambda$  is a proxy of relative excitation-inhibition (EI) balance.<sup>10</sup>

303 However, even glutamatergic synaptic inputs due to NMDA receptors can also be very slow.  
304 Therefore, it is also possible that increased  $\lambda$  may indicate a relative increase in the NMDA type  
305 synaptic currents. In the context of our results, we found that  $\lambda$  in PD is increased in the sensory  
306 areas. These areas usually have relatively small fractions of NMDA receptors.<sup>38</sup>

307 Finally, it is also possible that the change in  $\lambda$  is simply a reflection of changes in the dynamics  
308 of local and external inputs to the network. That is, if the network is driven by slowly fluctuating  
309 inputs it will also reflect in slower fluctuations and therefore larger  $\lambda$ . If this is the case then we

310 would also expect a change in the time scales of spiking activity.

## 311 **Hypotheses about network level changes in PD**

312 Each of these possibilities suggest a different but testable hypothesis. If the slope of the MEG  
313 reflects change in the relative fraction of excitatory and inhibitory currents, then it is tempting to  
314 hypothesise that in PD there is an increase in inhibition in the sensory region. Increase in relative  
315 fraction of NMDA will also account for an altered excitation-inhibition balance on longer time  
316 scales. Techniques such as MRS could be used for a non-invasive estimate of the relative fraction  
317 of AMPA, NMDA and GABA in order to test this hypothesis. Ideally, these hypotheses should be  
318 tested in animal models with *in vivo* measurements of excitatory and inhibitory currents.

319 If changes in the  $\lambda$  reflect a change in the time scales of fluctuations in the input then, we will  
320 need to explain how in a presynaptic network the spectrum of neuronal activity could change. For  
321 that we again revert to the hypothesis of a change in excitation-inhibition balance. However, before  
322 following this line of reasoning, we need to estimate whether there are significant changes in the  
323 spiking activity of a given brain region where  $\lambda$  has changed. This suggests that spiking activity  
324 from early sensory regions should also be recorded in animal models of PD.

325 As we discussed earlier, it is tempting to relate the slope of the frequency spectrum to EI bal-  
326 ance. Origin of pathological activity in the basal ganglia during PD, especially the beta band  
327 oscillations is closely related to changes in the EI balance in STN and GPe regions of the basal  
328 ganglia.<sup>39,40</sup> Local field potential recorded from the STN or GPe during DBS surgery can be used  
329 to estimate relative EI balance at different locations in the STN in terms of  $\lambda$ s. Such an estimate of  
330 relative EI balance could guide stimulation electrode placement.

## 331 **Age and UPDRS-III dependence**

332 A lack of a clear correlation between  $\lambda$ s and UPDRS-III suggests that it may not be useful as a  
333 clinical biomarker. However, correlation between  $\lambda$ s and age in the PD group suggests that  $\lambda$  is  
334 indeed altered in PD. In particular, we observe a positive correlation in PD in most brain regions

335 except the frontal regions. This result may suggest that dopamine depletion has an important impact  
336 on the sensory and motor 'ageing'.

337 A positive correlation between  $\lambda$  and age in PD patients is a curious observation. Previous work  
338 from several groups have shown a negative correlation between  $\lambda$  and age in the neocortex.<sup>41-43</sup>  
339 However, in over 60 years old HC,  $\lambda$  from somatosensory regions may positively correlate.<sup>44</sup> In  
340 contrast to these findings, in our data we did not observe any significant correlation between  $\lambda$  and  
341 age in HC. As age is highly (positively) correlated to disease duration, PD thus seems to affect all  
342 (except frontal parts) necortex's  $\lambda$ s by increasing them over age/disease duration.

### 343 **Effect of dopamine on $\lambda$**

344 Levodopa effects are fast as shown by the UPDRS-III score improvements only one hour after the  
345 drug administration. We found that in our data Levodopa influenced the spectral slowing. However,  
346 the effect of Levodopa on  $\lambda$  was not observed in the neocortex. To the best of our knowledge, there  
347 is no consensus on the cortical effects of Levodopa.<sup>36</sup> In our study, a possible reason could be the  
348 short time (1 hour) between taking the medication and recording of MEG. A recent study by Wang  
349 et al.<sup>13</sup> reported changes in the  $\lambda$  estimated from EEG. In that study, PD patient ON medication took  
350 their medication dose as usual, in the morning before the measurement. However, Wang et al.<sup>13</sup>  
351 also reported that Levodopa did not improve the aperiodic part (i.e.  $\lambda$  increased) of the neocortex  
352 activity spectrum. In addition, the total washout of Levodopa may take days.<sup>45</sup> The latter could  
353 explain the similar results we obtained for ON and OFF medication.

### 354 **Limitations**

355 Here we used a commonly used range of frequencies (1 to 45 Hz) for our analysis. This range is  
356 relatively small. Indeed the broader the frequency range, the better the fit should be. However,  
357 for MEG it is not as easy to take the largest band possible because muscle artifacts become more  
358 prominent in high frequencies. Therefore, local field potential or ECoG may be more suited for  
359 such an analysis over broad frequency ranges.

360 Next, we have used a specific brain atlas and it is not clear how the topography of  $\lambda$  may change  
361 when using a different brain atlas. In this regard, adding information from the sensor space may  
362 help matching the different atlases' results.

363 Finally, to better understand the functional implications of  $\lambda$  changes, a more detailed corre-  
364 lation analysis is needed that takes into account the UPDRS-III sub-scale<sup>46</sup> as well as cognitive  
365 scores.

366 **Implications**

367 Our findings also raise the question why frontal regions are more protected than sensory and mo-  
368 tor regions even though dopaminergic projections in the neocortex are primarily restricted to the  
369 frontal regions.<sup>47</sup> The lack of prefrontal changes between PD and HC may be due to dopamine  
370 pathways. Indeed, the main brain area producing dopamine and projecting to the cortex (in par-  
371 ticular prefrontal cortex) is the Ventral Tegmental Area, which is altered after the substantia nigra  
372 compacta in PD.<sup>48</sup> Hence, changes in the frontal regions may take longer to manifest.

373 In addition, because there is such a big change in the  $\lambda$  value in sensory regions one would ex-  
374 pect deficits in the sensory representations. It is well established that PD patients have olfactory,<sup>49</sup>  
375 proprioceptive<sup>50</sup> and cross-modal sensory fusion deficits.<sup>51</sup> However, our work suggest changes in  
376 other sensory modalities such as vision and audition.

377 It is common to measure functional connectivity between brain regions in a frequency depen-  
378 dent manner. Usually these estimates are based on filtered time series. Here we found that  $\lambda$  varies  
379 over time. Therefore, we can ask whether  $\lambda$  variations across brain regions are correlated or not  
380 in PD and HCs. Recent work suggests that functional connectivity based on the component of  
381 aperiodic activity may be more robust.<sup>52</sup>

382 Overall, we show that the aperiodic activity, which usually has been considered as noise, gives  
383 new insights in PD and deserves more attention when analysing any neural field potentials like  
384 ECoG, LFP, EEG and MEG. Finally, previous studies showed frequency slowing in relation to  
385 cognitive decline rather than the motor symptoms.<sup>5</sup> It could then be that the change in  $\lambda$  is a more

386 general expression of neurodegeneration than only the dopamine affected systems.

## 387 **Acknowledgements**

388 We thank Archishman Biswas for his help on the Figure S1.

## 389 **Funding**

390 Partial funding from StratNeuro (to AK), Swedish Research Council (to AK) and Digital Futures  
391 (to AK and PH), The Swedish Foundation for Strategic Research SBE 13-0115 (to DL, PS and  
392 MCV) is gratefully acknowledged.

393 The NatMEG facility is supported by Knut and Alice Wallenberg (grant #KAW2011.0207)

## 394 **Competing interests**

395 The authors report no competing interests.

## 396 Supplementary Material

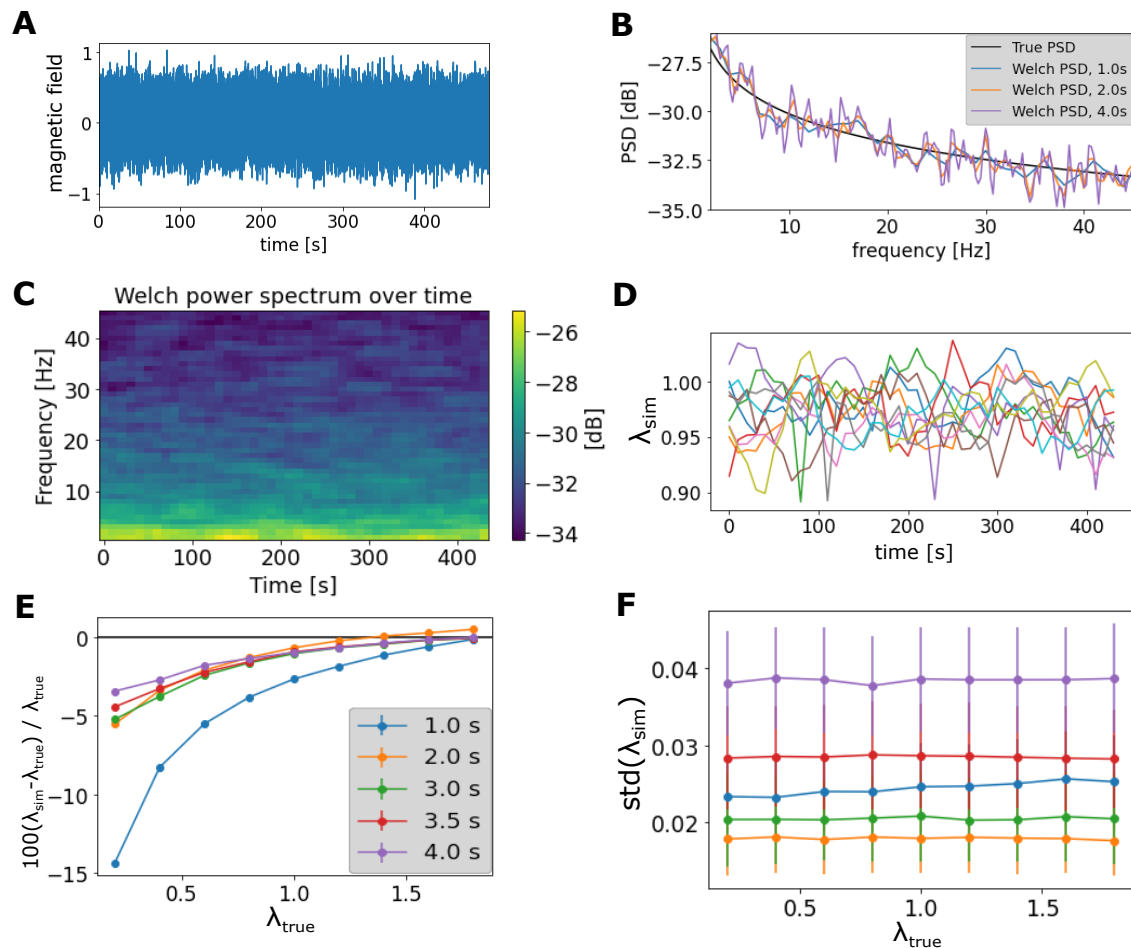


**Figure S1: Comparing the true 1/f-exponent of a simulated signal reconstructed from a given power spectrum of the form  $\kappa/f^\lambda$**  (A) Reconstructed signal from PSD equals to  $10^{-2.5}/f^{0.5}$ . (B) PSD of the reconstructed signal using the entire signal or a segment of it of sizes 1, 2 or 4 sec. (C) Spectrogram of the reconstructed signal shown in A using the method described in Materials and methods. (D) Temporal dynamics of  $\lambda_{sim}$  the reconstructed signals for a PSD  $10^{-2.5}/f^1$  and epochs of 1 sec. (E) Temporal average of  $\lambda$  from reconstructed signals,  $\lambda_{sim}$ , compared to the true  $\lambda_{true}$ . (F) Temporal standard deviation of  $\lambda$  from reconstructed signals in function of the true  $\lambda$ .

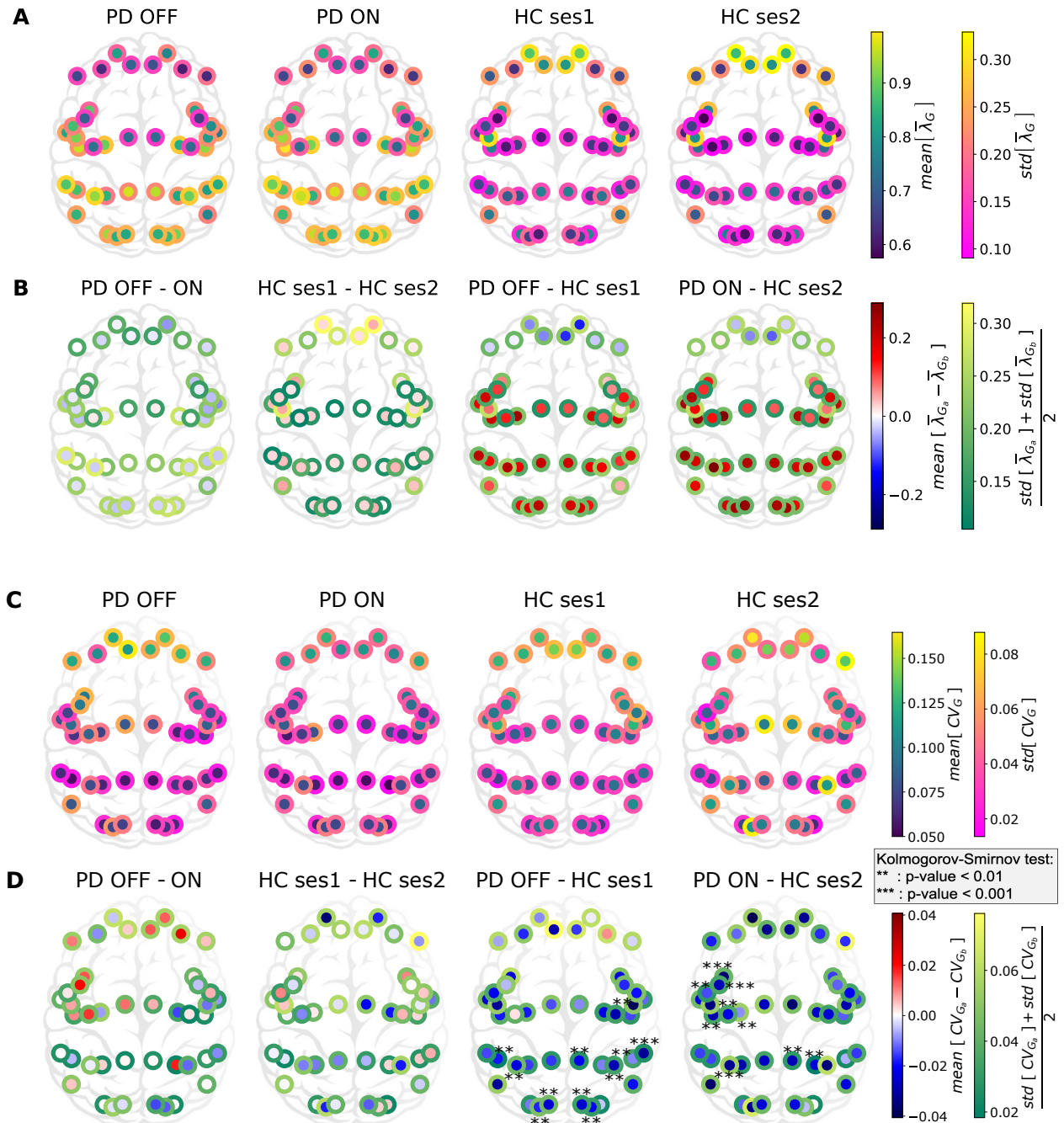


**Figure S2: Cortex-wide distribution of the mean and the coefficient of variation over time of  $\lambda$  within each group.** (A) (resp. (C)) Temporal mean (resp. coefficient of variation) of  $\lambda_G$  for each group  $G \in \{\text{HC ses1}, \text{HC ses2}, \text{PD-ON}, \text{PD-PFF}\}$ . The inside colour refers to the mean over the group. The border colour refers to the fluctuation of  $\bar{\lambda}_G$  (resp.  $CV_{\lambda_G}$ ) within the group  $G$ . (B) (resp. (D)) Temporal mean (resp. coefficient of variation) of  $\lambda$  between two groups  $G_a, G_b \in \{\text{HC ses1}, \text{HC ses2}, \text{PD-ON}, \text{PD-PFF}\}$ . The inside colour refers to the difference between the means over the groups. The border colour refers to the averaged fluctuation of  $\bar{\lambda}_G$  (resp.  $CV_{\lambda_G}$ ) combining the two groups  $G_a$  and  $G_b$ .

Patient Brain region \	PD ON lh	PD ON rh	PD OFF lh	PD OFF rh
AC-MPC	0,052655	0,0327	0,023435	0,05004
AAC	0,005475	0,008165	0,001995	0,01079
DSVC	0,00098	0,10805	0,001665	0,05319
DPC	0,029015	0,09365	0,020805	0,138505
EAC	0,00134	0,00813	0,00047	0,002055
EVC	0,009255	0,00509	0,017115	0,016085
IFC	0,0169	0,11816	0,065705	0,072345
IPC	0,004815	0,014195	0,00435	0,006125
I-FOC	0,001375	0,00364	0,00146	0,002615
LTC	0,00621	0,00102	0,0191	0,01329
MT+C-NVA	0,00308	0,0098	0,004235	0,00613
MTC	0,001795	0,004075	0,008265	0,00591
O-PFC	0,05662	0,15312	0,061315	0,053295
PL-MCC	0,0401	0,02616	0,09309	0,02303
PCC	0,00078	0,007705	0,00162	0,006045
POC	0,015555	0,04716	0,012155	0,02366
PMC	0,018335	0,100665	0,12863	0,05784
PVC-V1	0,01139	0,00877	0,024695	0,00548
SMC	0,025775	0,033375	0,10384	0,02987
SPC	0,001025	0,0362	0,003105	0,014585
T-P-O-J	0,000495	0,006065	0,002675	0,0031
VSVC	0,00903	0,001855	0,00938	0,009635

**Table S1: P-values of the distance correlation per brain region, PD patient session and hemisphere.** The shaded cells are the 20 lowest p-values.

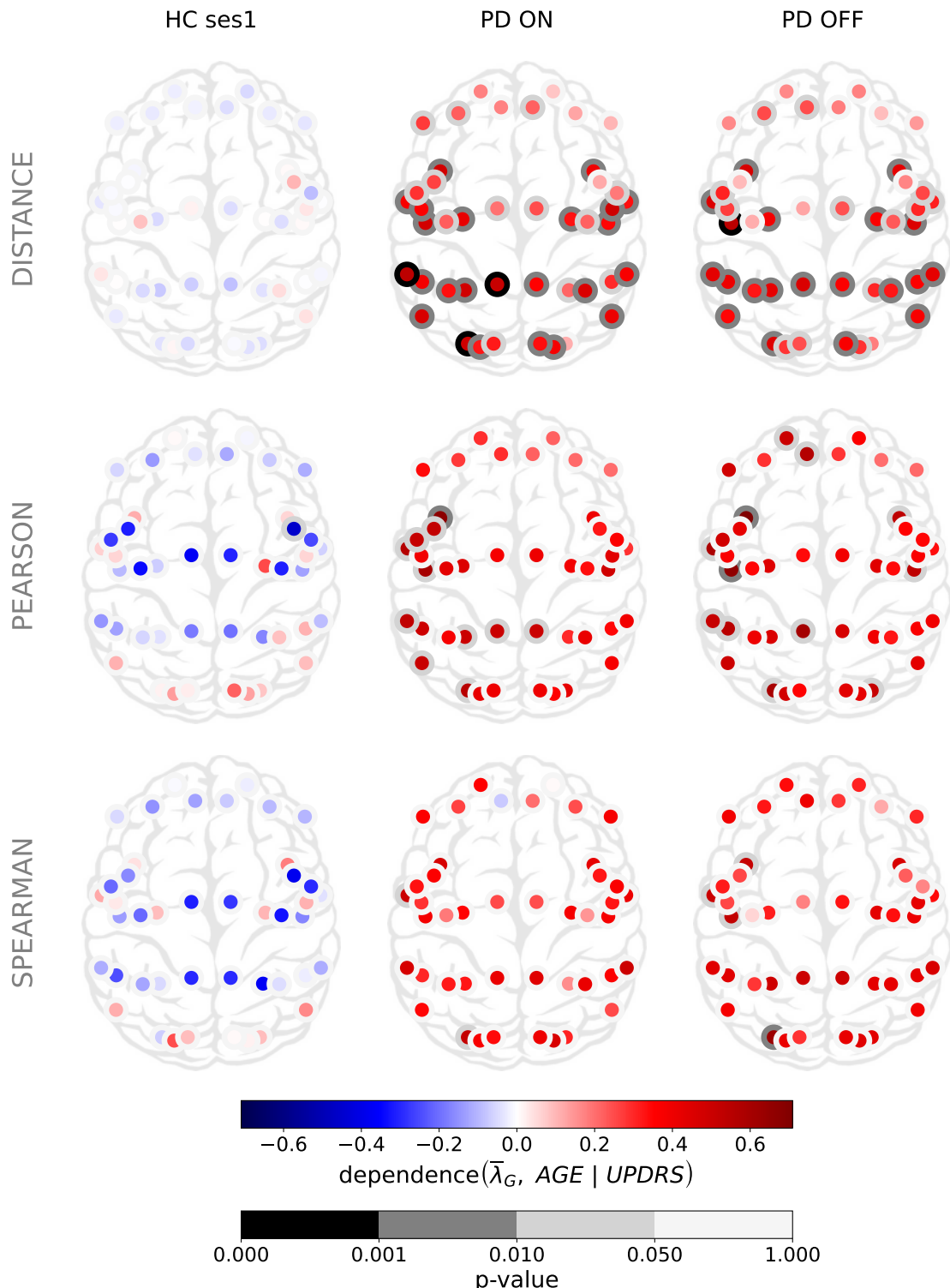


**Figure S3: Cortex-wide distribution of different relationship measures between the mean over time of  $\lambda$  and ages within each group.**

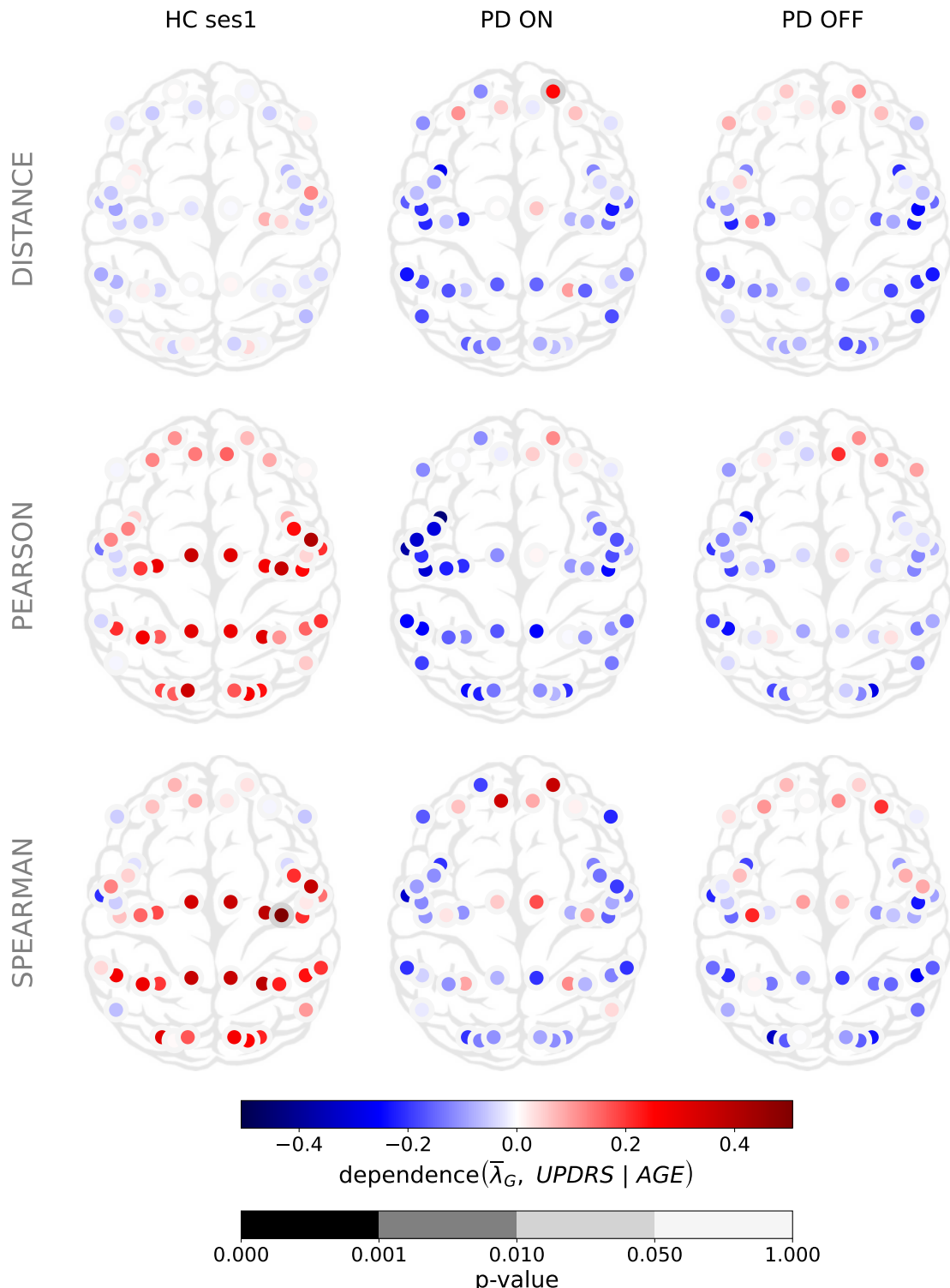


**Figure S4:** Cortex-wide distribution of different relationship measures between the mean over time of  $\lambda$  and UPDRS-III within each PD group and combining them (first column).

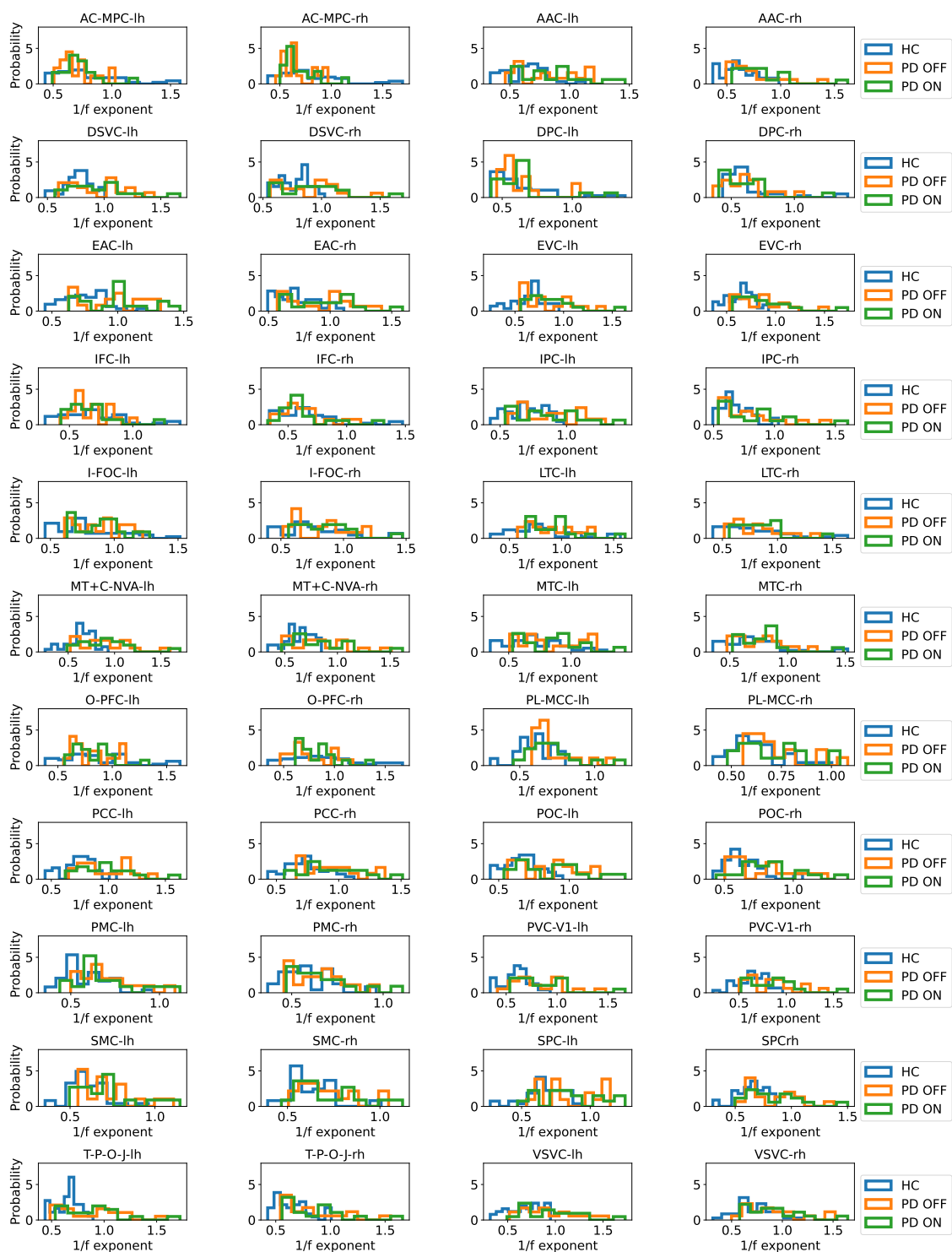


**Figure S5:  $1/f$ -exponent distributions over the different groups in the different BRs.**

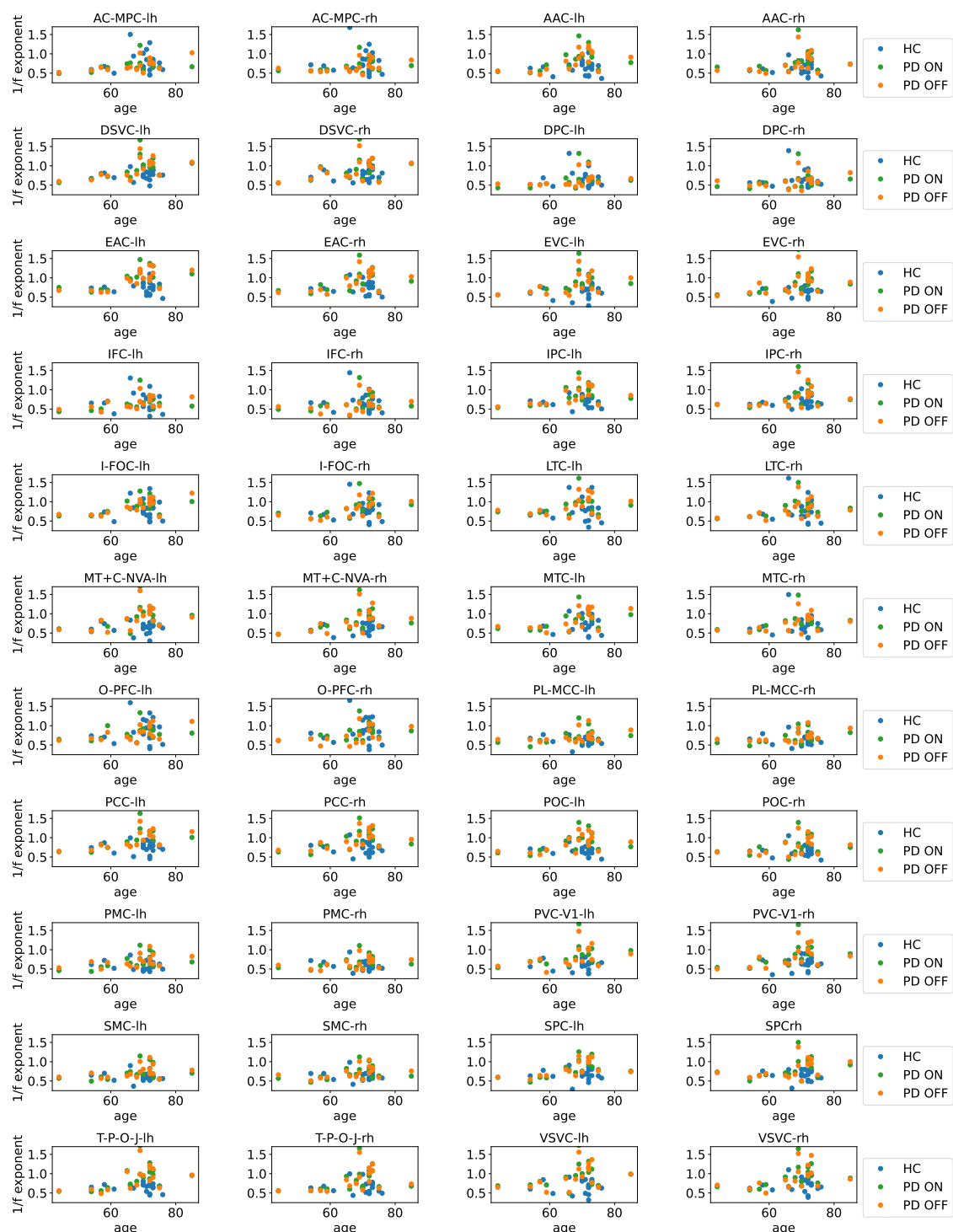


**Figure S6:  $1/f$ -exponent as a function of age for the different groups in the different BRs.**

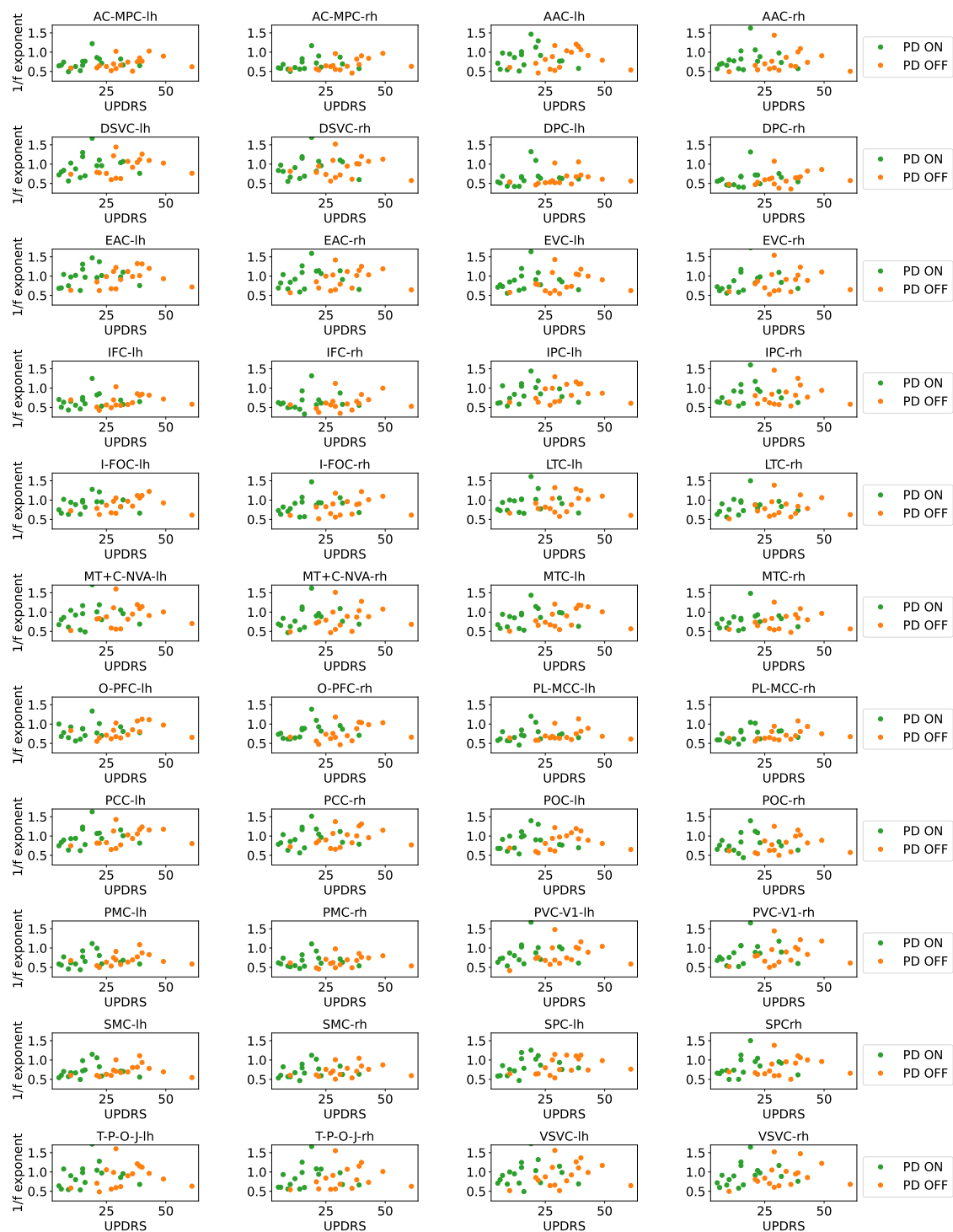


**Figure S7:  $1/f$ -exponent as a function of UPDRS-III for PD-ON and PD-OFF in the different BRs.**

## 397 References

- 398 [1] M. M. McGregor and A. B. Nelson. “Circuit Mechanisms of Parkinson’s Disease”. *Neuron*  
399 101.6 (2019), pp. 1042–1056.
- 400 [2] V. J. Geraedts, L. I. Boon, J. Marinus, et al. “Clinical correlates of quantitative EEG in  
401 Parkinson disease: A systematic review”. *Neurology* 91.19 (2018), pp. 871–883.
- 402 [3] L. I. Boon, V. J. Geraedts, A. Hillebrand, et al. “A systematic review of MEG-based studies  
403 in Parkinson’s disease: The motor system and beyond”. *Human Brain Mapping* 40.9 (2019),  
404 pp. 2827–2848.
- 405 [4] J. Bosboom, D. Stoffers, C. Stam, et al. “Resting state oscillatory brain dynamics in Parkin-  
406 son’s disease: an MEG study”. *Clinical Neurophysiology* 117.11 (2006), pp. 2521–2531.
- 407 [5] K. T. O. Dubbelink, D. Stoffers, J. B. Deijen, J. W. Twisk, C. J. Stam, and H. W. Berendse.  
408 “Cognitive decline in Parkinson’s disease is associated with slowing of resting-state brain  
409 activity: a longitudinal study”. *Neurobiology of aging* 34.2 (2013), pp. 408–418.
- 410 [6] D. Stoffers, J. Bosboom, J. Deijen, E. C. Wolters, H. Berendse, and C. Stam. “Slowing of  
411 oscillatory brain activity is a stable characteristic of Parkinson’s disease without dementia”.  
412 *Brain* 130.7 (2007), pp. 1847–1860.
- 413 [7] D. Stoffers, J. L. Bosboom, J. B. Deijen, E. C. Wolters, C. J. Stam, and H. W. Berendse. “In-  
414 creased cortico-cortical functional connectivity in early-stage Parkinson’s disease: an MEG  
415 study”. *Neuroimage* 41.2 (2008), pp. 212–222.
- 416 [8] K. T. O. Dubbelink, D. Stoffers, J. B. Deijen, et al. “Resting-state functional connectivity as  
417 a marker of disease progression in Parkinson’s disease: A longitudinal MEG study”. *Neu-  
418 roImage: Clinical* 2 (2013), pp. 612–619.
- 419 [9] C. Hammond, H. Bergman, and P. Brown. “Pathological synchronization in Parkinson’s dis-  
420 ease: networks, models and treatments”. *Trends in neurosciences* 30.7 (2007), pp. 357–364.

- 421 [10] R. Gao, E. J. Peterson, and B. Voytek. “Inferring synaptic excitation/inhibition balance from  
422 field potentials”. *Neuroimage* 158 (2017), pp. 70–78.
- 423 [11] M. C. Vinding, A. Eriksson, C. M. T. Low, et al. “Different features of the cortical sen-  
424 sorimotor rhythms are uniquely linked to the severity of specific symptoms in Parkinson’s  
425 disease”. *medRxiv* (2021).
- 426 [12] A. I. Wiesman, J. da Silva Castanheira, C. Degroot, et al. “A sagittal gradient of pathological  
427 and compensatory effects of neurophysiological slowing in Parkinson’s disease”. *medRxiv*  
428 (2022).
- 429 [13] Z. Wang, Y. Mo, Y. Sun, et al. “Separating the aperiodic and periodic components of neural  
430 activity in Parkinson’s disease”. *European Journal of Neuroscience* 56.6 (2022), pp. 4889–  
431 4900.
- 432 [14] M. Vinding, P. Tsitsi, J. Waldthaler, et al. “Reduction of spontaneous cortical beta bursts  
433 in Parkinson’s disease is linked to symptom severity”. *Brain Communications* 2.1 (2020),  
434 fcaa052.
- 435 [15] A. M. Dale, A. K. Liu, B. R. Fischl, et al. “Dynamic statistical parametric mapping: com-  
436 bining fMRI and MEG for high-resolution imaging of cortical activity”. *neuron* 26.1 (2000),  
437 pp. 55–67.
- 438 [16] A. Gramfort, M. Luessi, E. Larson, et al. “MEG and EEG data analysis with MNE-Python”.  
439 *Frontiers in neuroscience* (2013), p. 267.
- 440 [17] M. F. Glasser, T. S. Coalson, E. C. Robinson, et al. “A multi-modal parcellation of human  
441 cerebral cortex”. *Nature* 536.7615 (2016), pp. 171–178.
- 442 [18] P. Welch. “The use of fast Fourier transform for the estimation of power spectra: A method  
443 based on time averaging over short, modified periodograms”. *IEEE Transactions on Audio  
444 and Electroacoustics* 15.2 (1967), pp. 70–73.

- 445 [19] T. Donoghue, M. Haller, E. J. Peterson, et al. “Parameterizing neural power spectra into  
446 periodic and aperiodic components”. *Nature neuroscience* 23.12 (2020), pp. 1655–1665.
- 447 [20] G. J. Székely, M. L. Rizzo, and N. K. Bakirov. “Measuring and testing dependence by cor-  
448 relation of distances”. *The Annals of Statistics* 35.6 (2007).
- 449 [21] G. J. Székely and M. L. Rizzo. “Partial distance correlation with methods for dissimilarities”.  
450 *The Annals of Statistics* 42.6 (2014), pp. 2382–2412.
- 451 [22] J. L. Hodges. “The significance probability of the Smirnov two-sample test”. *Arkiv för  
452 Matematik* 3.5 (1958), pp. 469–486.
- 453 [23] T. J. Collier, N. M. Kanaan, and J. H. Kordower. “Aging and Parkinson’s disease: different  
454 sides of the same coin?” *Movement Disorders* 32.7 (2017), pp. 983–990.
- 455 [24] J. Waldthaler, P. Tsitsi, and P. Svenningsson. “Vertical saccades and antisaccades: comple-  
456 mentary markers for motor and cognitive impairment in Parkinson’s disease”. *npj Parkinson’s Disease* 5.1 (2019), pp. 1–6.
- 457 [25] R. A. Armstrong. “Visual dysfunction in Parkinson’s disease”. *International review of neu-  
459 robiology* 134 (2017), pp. 921–946.
- 460 [26] S. Dave, T. Brothers, and T. Swaab. “1/f neural noise and electrophysiological indices of  
461 contextual prediction in aging”. *Brain Research* 1691 (2018), pp. 34–43.
- 462 [27] M. A. Colombo, M. Napolitani, M. Boly, et al. “The spectral exponent of the resting EEG  
463 indexes the presence of consciousness during unresponsiveness induced by propofol, xenon,  
464 and ketamine”. *NeuroImage* 189 (2019), pp. 631–644.
- 465 [28] J. D. Lendner, R. F. Helfrich, B. A. Mander, et al. “An electrophysiological marker of arousal  
466 level in humans”. *eLife* 9 (2020), e55092.
- 467 [29] J. Weber, T. Klein, and V. Abeln. “Shifts in broadband power and alpha peak frequency  
468 observed during long-term isolation”. *Scientific Reports* 10.1 (2020), p. 17987.

- 469 [30] J. L. Molina, B. Voytek, M. L. Thomas, et al. “Memantine Effects on Electroencephalographic Measures of Putative Excitatory/Inhibitory Balance in Schizophrenia”. *Biological Psychiatry: Cognitive Neuroscience and Neuroimaging* 5.6 (2020), pp. 562–568.
- 470
- 471
- 472 [31] L. Waschke, T. Donoghue, L. Fiedler, et al. “Modality-specific tracking of attention and sensory statistics in the human electrophysiological spectral exponent”. *eLife* 10 (2021), e70068.
- 473
- 474
- 475 [32] J. Q. Kosciessa, U. Lindenberger, and D. D. Garrett. “Thalamocortical excitability modulation guides human perception under uncertainty”. *Nature Communications* 12.1 (2021), p. 2430.
- 476
- 477
- 478 [33] B. D. Oslund, B. R. Alperin, T. Drew, and S. L. Karalunas. “Behavioral and cognitive correlates of the aperiodic (1/f-like) exponent of the EEG power spectrum in adolescents with and without ADHD”. *Developmental Cognitive Neuroscience* 48 (2021), p. 100931.
- 479
- 480
- 481 [34] Z. R. Cross, A. W. Corcoran, M. Schlesewsky, M. J. Kohler, and I. Bornkessel-Schlesewsky. “Oscillatory and Aperiodic Neural Activity Jointly Predict Language Learning”. *Journal of Cognitive Neuroscience* (2022), pp. 1–20.
- 482
- 483
- 484 [35] J. Zhang, A. Villringer, and V. V. Nikulin. “Dopaminergic Modulation of Local Non-oscillatory Activity and Global-Network Properties in Parkinson’s Disease: An EEG Study”. *Frontiers in Aging Neuroscience* 14 (2022).
- 485
- 486
- 487 [36] M. C. Vinding, A. Eriksson, C. M. Ting Low, et al. “Changes in non-oscillatory features of the cortical sensorimotor rhythm in Parkinson’s disease across age”. *medRxiv* (2022).
- 488
- 489 [37] M. Hämäläinen, R. Hari, R. J. Ilmoniemi, J. Knuutila, and O. V. Lounasmaa. “Magnetoencephalography—theory, instrumentation, and applications to noninvasive studies of the working human brain”. *Reviews of modern Physics* 65.2 (1993), p. 413.
- 490
- 491
- 492 [38] X.-J. Wang. “Macroscopic gradients of synaptic excitation and inhibition in the neocortex”. *Nature Reviews Neuroscience* 21.3 (2020), pp. 169–178.
- 493

- 494 [39] A. Kumar, S. Cardanobile, S. Rotter, and A. Aertsen. “The role of inhibition in generating  
495 and controlling Parkinson’s disease oscillations in the basal ganglia”. *Frontiers in systems*  
496 *neuroscience* 5 (2011), p. 86.
- 497 [40] J. Bahuguna, A. Sahasranamam, and A. Kumar. “Uncoupling the roles of firing rates and  
498 spike bursts in shaping the STN-GPe beta band oscillations”. *PLoS computational biology*  
499 16.3 (2020), e1007748.
- 500 [41] A. J. Finley, D. J. Angus, C. M. Van Reekum, R. J. Davidson, and S. M. Schaefer. “Periodic  
501 and aperiodic contributions to theta-beta ratios across adulthood”. *Psychophysiology* 59.11  
502 (2022), e14113.
- 503 [42] A. Merkin, S. Sghirripa, L. Graetz, et al. “Do age-related differences in aperiodic neural ac-  
504 tivity explain differences in resting EEG alpha?” *Neurobiology of Aging* 121 (2023), pp. 78–  
505 87.
- 506 [43] A. E. Smith, A. Chau, D. Greaves, H. Keage, and D. C. Feuerriegel. “Resting EEG power  
507 spectra across middle to late life: Associations with age, cognition, APOE-ε4 carriage and  
508 cardiometabolic burden”. *bioRxiv* (2022).
- 509 [44] B. Brady and T. Bardouille. “Periodic/Aperiodic parameterization of transient oscillations  
510 (PAPTO)–Implications for healthy ageing”. *NeuroImage* 251 (2022), p. 118974.
- 511 [45] R. A. Hauser and N. H. Holford. “Quantitative description of loss of clinical benefit fol-  
512 lowing withdrawal of levodopa–carbidopa and bromocriptine in early Parkinson’s disease”.  
513 *Movement disorders: official journal of the Movement Disorder Society* 17.5 (2002), pp. 961–  
514 968.
- 515 [46] C. G. Goetz, B. C. Tilley, S. R. Shaftman, et al. “Movement Disorder Society-sponsored re-  
516 vision of the Unified Parkinson’s Disease Rating Scale (MDS-UPDRS): Scale presentation  
517 and clinimetric testing results: MDS-UPDRS: Clinimetric Assessment”. *Movement Disor-  
518 ders* 23.15 (2008), pp. 2129–2170.

- 519 [47] M. Le Moal and H. Simon. “Mesocorticolimbic dopaminergic network: functional and reg-  
520 ulatory roles”. *Physiological reviews* 71.1 (1991), pp. 155–234.
- 521 [48] W. Dauer and S. Przedborski. “Parkinson’s Disease: Mechanisms and Models”. *Neuron* 39.6  
522 (2003), pp. 889–909.
- 523 [49] N. Quinn, M. Rossor, and C. Marsden. “Olfactory threshold in Parkinson’s disease.” *Journal*  
524 *of Neurology, Neurosurgery & Psychiatry* 50.1 (1987), pp. 88–89.
- 525 [50] J. Konczak, D. M. Corcos, F. Horak, et al. “Proprioception and motor control in Parkinson’s  
526 disease”. *Journal of motor behavior* 41.6 (2009), pp. 543–552.
- 527 [51] S. Hwang, P. Agada, S. Grill, T. Kiemel, and J. J. Jeka. “A central processing sensory deficit  
528 with Parkinson’s disease”. *Experimental brain research* 234.8 (2016), pp. 2369–2379.
- 529 [52] A. Ibarra Chaoul and M. Siegel. “Cortical correlation structure of aperiodic neuronal popu-  
530 lation activity”. *NeuroImage* 245 (2021), p. 118672.